PERSPECTIVE

Dalton
www.rsc.org/dalton

Interpreting and controlling the structures of six-coordinate copper(II) centres – When is a compression *really* a compression?†

Malcolm A. Halcrow*
School of Chemistry, University of Leeds, Woodhouse Lane, Leeds, UK LS2 9JT.
E-mail: M.A.Halcrow@chem.leeds.ac.uk

Received 5th August 2003, Accepted 19th September 2003
First published as an Advance Article on the web 8th October 2003

Many experimental observations of 'inverse' or 'quenched' Jahn–Teller effects in copper(II) compounds in fact reflect a normal Jahn–Teller-elongated configuration that is masked by structural disorder. On the other hand, a small number of copper(II) complexes are known that genuinely exhibit these unusual structures. It requires careful interpretation of spectroscopic and structural data to distinguish these two scenarios.

Introduction

Copper(II) is the most studied of all the transition metal ions. For example, in July 2003 the combined number of Cu(II) compounds on the inorganic structure database,[1] and the Cambridge crystallographic database,[2] was 13 604. This is 66% more than for the next most ubiquitous transition ion, which is Ni(II) with 8182 structures. Quite apart from the biological[3,4] or technological[4–6] relevance of Cu(II) compounds, the attractions of Cu(II) to inorganic chemistry researchers are easy to understand, given the user-friendliness of Cu(II) compounds. These are commonly air- and moisture-stable, have informative and easy-to-obtain UV/vis[7] and EPR[8,9] spectroscopic signatures, and often undergo reactions in solution effectively within time of mixing. The stereochemical flexibility of Cu(II) compounds also means that they adopt a wider range of coordination geometries than for any other transition ion.[9]

Many of the attributes listed above are consequences of the d^9 configuration of the Cu(II) ion. In particular, in symmetries like O_h or T_d where the odd d-electron occupies a degenerate d-orbital set, Cu(II) compounds are subject to Jahn–Teller distortions.[10] The paradigm is the octahedral case, where the Jahn–Teller theorem splits the degeneracy of the ^2E_g ground state, reflecting a concomitant elongation or compression of the Cu–ligand bonds parallel to one of the three molecular axes (Scheme 1). While both distortions are possible, Jahn–Teller elongations are preferred owing to $4s-3d_{z^2}$ orbital mixing, which slightly lowers the energy of $3d_{z^2}$ compared to $3d_{x^2-y^2}$. This additional stabilisation is greater in a Jahn–Teller-elongated Cu(II) ion (where $3d_{z^2}$ contains two electrons), than in a Jahn–Teller-compressed one (where it only contains one).[11]

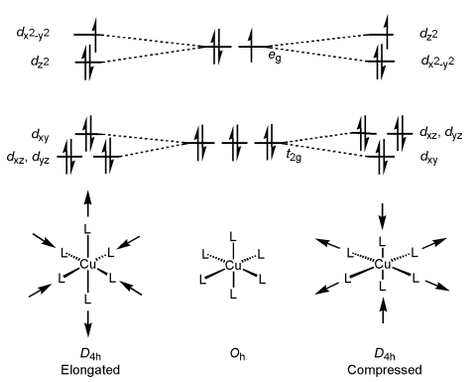

Scheme 1 Diagram showing the two possible Jahn–Teller splittings of the d-energy levels in an octahedral $[CuL_6]^{2+}$ complex, and the structural distortions that result from them.

Strictly speaking, the above argument only applies to six-coordinate complexes with true O_h symmetry, where all six ligands and all three molecular axes, are the same. There is a more numerous class of compounds of type *cis*- or *trans*-$[CuX_2L_4]$, which also typically undergo a structural elongation along one of the two degenerate molecular axes (Scheme 2).[9,12] This is commonly termed a 'pseudo-Jahn–Teller' distortion, because if the compounds were not distorted they would still not possess d-orbital degeneracy.[9] It is caused by vibronic coupling of non-degenerate, but close-in-energy, $d_{x^2-y^2}$ and d_{z^2} energy levels, and is a second-order Jahn–Teller phenomenon.[13] The structural and spectroscopic characteristics of Jahn–Teller and pseudo-Jahn–Teller distortions are essentially similar, and the term 'Jahn–Teller' is used generically in this article to refer to both types of distortion unless otherwise stated.

There is only one known class of six-coordinate Cu(II) compound that apparently exhibits no Jahn–Teller distortion under ambient conditions, namely β-$CuX_2(NH_3)_2$ (X^- = Cl^- or Br^-; see later). There is also a handful of Cu(II) compounds where the Jahn–Teller effect causes a compressed, rather than an elongated, octahedral structure. However, static or fluxional disorder of a Jahn–Teller axis of elongation can have a pro-

† Electronic supplementary information (ESI) available: a table of compounds whose apparently anomalous crystallographic co-ordination geometries are a result of Jahn–Teller disorder, and the techniques used to resolve this question. See http://www.rsc.org/suppdata/dt/b3/b309242a/

Malcolm Halcrow obtained his PhD at the University of Edinburgh, under Prof. Martin Schröder. He then undertook post-doctoral work in the Laboratoire de Chimie de Coordination du CNRS (Toulouse) with Dr Bruno Chaudret, and at Indiana University with Prof. George Christou. After four years as a Royal Society Research Fellow at the University of Cambridge, in 1998 he moved to the University of Leeds where he is now Lecturer. His research interests involve the design, synthesis and physical characterisation of new copper enzyme models, and of functional molecule-based transition metal switches or magnets. He has co-authored 95 research publications.

Malcolm A. Halcrow

DOI: 10.1039/b309242a

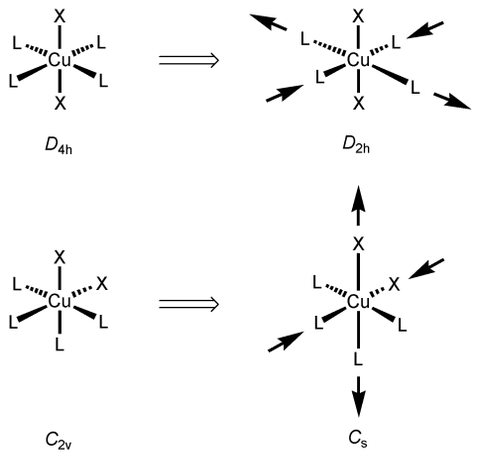

Scheme 2 Pseudo-Jahn–Teller distortions in *cis*- and *trans*-$[CuX_2L_4]^{2+}$ complexes.

found and misleading effect on the crystallographic and spectroscopic properties of a Cu(II) compound, which has often led to mis-assignments of structural distortions and/or electronic configurations in the literature. This article is intended to discuss these pitfalls, and how they can be avoided; to critically review six-coordinate Cu(II) compounds in the literature that have unusual (that is, not Jahn–Teller elongated) structures; and, to describe some of our own work in which, for the first time, we have been able to controllably obtain different types of structural distortion in molecular Cu(II) complexes. More detailed reviews of the physical chemistry of static and dynamic Jahn–Teller effects in transition metal chemistry have been published by others.[9,12–15]

Distinguishing between Jahn–Teller elongated and compressed structures

In principle, the detection of a Jahn–Teller elongation or compression at a metal centre should be straightforward. The 'long' and 'short' Cu–ligand bond lengths in a distorted octahedron typically differ by ≥20%, which is easily observed even at poor crystallographic resolution. In addition, elongated and compressed Cu(II) octahedra adopt different electronic ground states, with their unpaired electron occupying the $d_{x^2-y^2}$ or d_{z^2} atomic orbital respectively (hereafter written as $\{d_{x^2-y^2}\}^1$ or $\{d_{z^2}\}^1$; Scheme 1). These yield very different powder EPR spectra, whose lineshapes are diagnostic for which d-orbital in the molecule is singly occupied (Fig. 1).[8] For a $\{d_{x^2-y^2}\}^1$ complex, a $g_1 > g_2 \geq g_3 > 2.00$ pattern in the EPR spectrum is expected (Fig. 1(a)), while a $\{d_{z^2}\}^1$ configuration yields $g_1 \geq g_2 > g_3 \approx 2.00$ (Fig. 1(b)).[8,9] Different sequences of d–d absorptions in the UV/vis/NIR spectrum might also be expected from these two different d-orbital orderings.[16–19] However, static or dynamic librational disorder of a Jahn–Teller elongation in the solid state can lead to crystallographic bond lengths, *and* powder EPR spectra, that resemble instead those shown by a $\{d_{z^2}\}^1$ species with a compressed structure.[9,12,14,15,20] Comparable elongated and compressed octahedral Cu(II) species can also sometimes give very similar visible absorption spectra.[21] Hence, it can require more than the usual routine characterisation to unambiguously determine the electronic configuration and true molecular structure of a Cu(II) centre.

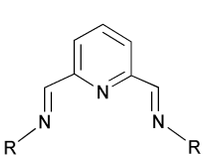

L^1R

R = Cy, *t*Bu, NH_2, OH

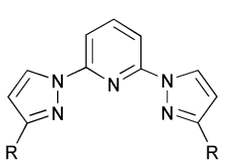

L^2R

R = H, *i*Pr, Ph, Mes, *t*Bu, CF_3

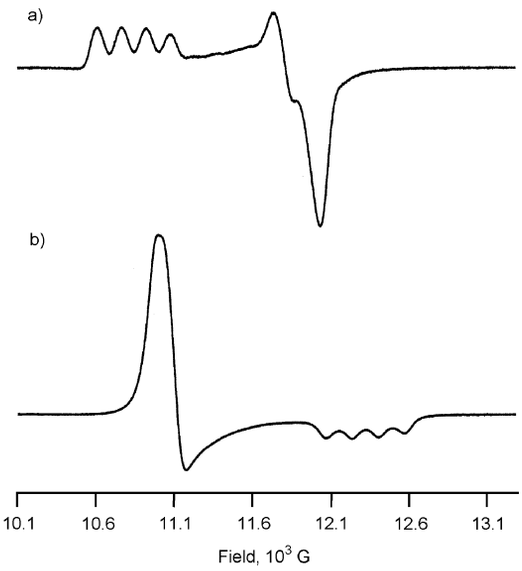

Fig. 1 Q-Band powder EPR spectra at 10 K of two complexes $[Cu(L^1R)_2][BF_4]_2$: (a) R = Cy, with a static $\{d_{x^2-y^2}\}^1$ pseudo-Jahn–Teller-elongated structure; and (b) R = *t*Bu with a $\{d_{z^2}\}^1$ compressed octahedral structure.[53] The four-line splitting on one line in each spectrum arises from hyperfine coupling to the Cu nucleus (^{63,65}Cu, $I = 3/2$).

Librational disorder of an axis of Jahn–Teller elongation in the crystal will lead to an apparent equalisation of the observed Cu–ligand bond lengths. If the disorder is dynamic, then the Cu–ligand bond lengths in the crystal will be temperature-dependent (Fig. 2).[12,14,15] Structure determinations at two

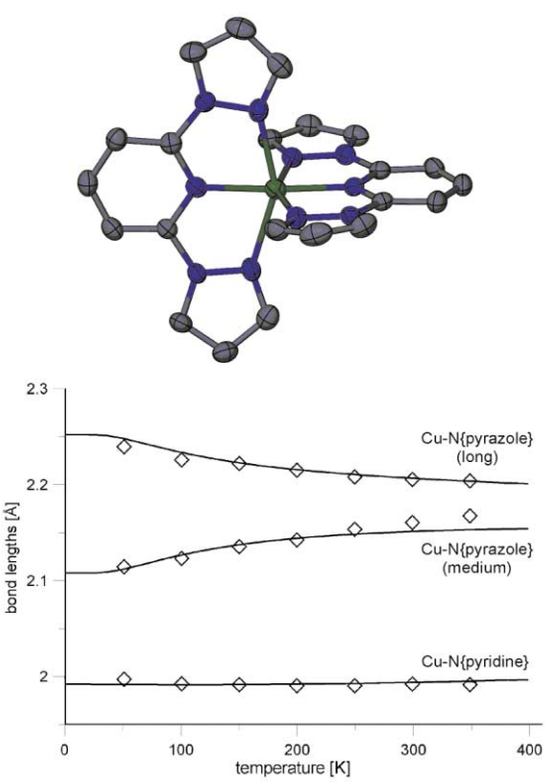

Fig. 2 View of the complex dication in the crystal structure of $[Cu(L^2H)_2][BF_4]_2$ at 150 K, and the temperature dependence of its Cu–N bond lengths in the range 50–350 K.[22,25] All H atoms have been omitted for clarity. The plotted distances are average values for each pair of short, medium and long Cu–N bonds in the rhombic copper coordination sphere, and the lines represent the best fit of these data to the Bürgi and Hitchman model of Jahn–Teller fluxionality. Colour code: C = grey, N = blue, Cu = green.

temperatures are enough to prove the existence of dynamic disorder. However, if several structures are obtained, the resultant data can be modelled to provide thermodynamic parameters for the Jahn–Teller distortion (Fig. 2). The Silver and Getz model treats the fluxionality as a simple two-state equilibrium.[23–25] Although computationally simple, this approach does not always successfully reproduce experimental observation; and, it can lead to unrealistic results if applied to sterically constrained metal–ligand systems.[25] More generally, Bürgi and Hitchman's method treats Jahn–Teller fluxionality as a set of coupled copper–ligand vibrational modes, and calculates the complete vibrational potential surface for the metal and donor atoms.[26,27] The same methods can be used to model variable-temperature single-crystal EPR data for fluxional $S = ½$ metal ions (see below).[23,28]

If, however, the Jahn–Teller disorder in a compound is static, and/or the Cu centre in the crystal lies on a special position, then its Cu–ligand bond lengths will be temperature-invariant. In that case, a thermal ellipsoid analysis is necessary to determine the presence or absence of librational disorder.[15] Unfortunately, such disorder along a metal–ligand bond is not always evident in the visible shape of the thermal ellipsoids of the atoms concerned. A much more sensitive way of detecting librational disorder in a structure is through a mean-square displacement amplitude (MSDA) analysis.[15,29] This extracts from the thermal ellipsoids the amplitude of vibration of an atom along each of the bonds it takes part in. The MSDA for a given atom, parallel to a given chemical bond, is given by eqn. (1):

$$\mathrm{MSDA} = \frac{\sum_{i=1}^{3}\sum_{j=1}^{3} U_{ij} n_i n_j}{\left|n\right|^2} \qquad (1)$$

where U_{ij} is an element of the 3 × 3 matrix of thermal parameters and n_i, n_j are elements of the vector describing the bond. The difference between the MSDA values for the two atoms in a given chemical bond (ΔMSDA) will then be proportional to the degree of interatomic libration along that bond (eqn. (2)).

$$\Delta\mathrm{MSDA} = \mathrm{MSDA(ligand)} - \mathrm{MSDA(metal)} \qquad (2)$$

The parameter ΔMSDA is often given the abbreviation $<d^2>$, with units of Å², but is also sometimes quoted as its square root $<d>$, whose units are then Å. All ΔMSDA data in this article are quoted as $<d^2>$. MSDA analyses can be carried out quickly from most standard crystallographic output files, when the atoms of interest have been refined anisotropically, using the program THMA11.[29] This is incorporated into the freely available PLATON[30,31] and WINGX[31,32] suites of crystallographic software. A MSDA calculation is also sometimes called a TLS analysis, after the symbols for three vector quantities that are involved in the calculation.[29]

As an example, Scheme 3 shows the crystallographic Cu–N bond lengths, and the corresponding $<d^2>$ values, for $[Cu(L^2H)_2][BF_4]_2$ (Fig. 2) at two temperatures.[22,33] At 300 K, the Cu–N bond lengths are highly rhombic, with an apparent structural compression along the two central Cu–N{pyridine} bonds.[22] However, there is a wide spread of $<d^2>$ values for the six Cu–N bonds, with $<d^2>$ for two of the distal Cu–N{pyrazole} bonds being particularly high. This clearly indicates the presence of librational disorder involving, at least, these two bonds (in fact, all four of the distal Cu–N{pyrazole} distances are temperature-dependent at $T \geq 50$ K, Fig. 2). Upon cooling to 31 K the Cu–N bond lengths have changed substantially, and now show a clear pseudo-Jahn–Teller elongation along one N{pyrazole}–Cu–N{pyrazole} axis.[33] Now, all six Cu–N bonds in the structure show similar and low $<d^2>$ values, consistent

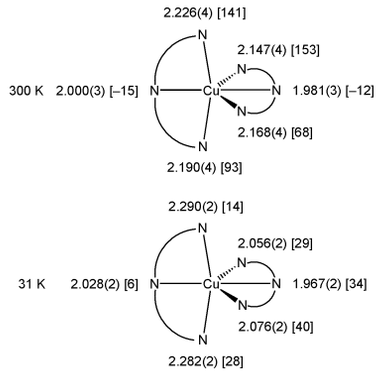

Scheme 3 Bond lengths (Å), and $<d^2>$ values ($\times 10^4$ Å²) in square brackets, for $[Cu(L^2H)_2][BF_4]_2$ (Fig. 2) at 300 K and 31 K.[22,33] Only one of the three independent molecules in the asymmetric unit of this compound at 31 K[33] is shown. The orientation of the molecule in these diagrams is the same as in Fig. 2.

with a static molecular structure.[22] Hence, the Jahn–Teller fluxionality present at 300 K has been frozen out at 31 K. The negative $<d^2>$ parameter shown by two of the Cu–N bonds at 300 K simply means that the Cu atom has a higher amplitude of vibration in the direction of those bonds than the N atom.

EXAFS can also be used to derive the 'true' Cu–ligand bond lengths in a disordered Jahn–Teller system. As a form of electronic spectroscopy, the EXAFS experiment has a shorter timescale than molecular vibrations.[34] Hence, EXAFS-derived bond lengths are uncontaminated by fluxionality, or any other disorder, that may be present in a crystal structure. EXAFS data have been used to reassign the crystal structures of several putatively Jahn–Teller compressed Cu(II) compounds as in fact showing a disordered structural elongation.[35–38]

Jahn–Teller disorder also strongly perturbs the solid-state EPR spectra of Cu(II) compounds. Librational or static disorder of the molecular axes of the unpaired spins in a sample can cause averaging of the corresponding g-values in the bulk material.[9,20] Hence, if the Jahn–Teller elongation is equally disordered over all six Cu–ligand bonds, a strictly or nearly isotropic powder EPR spectrum would result.[36,39–44] If it is equally disordered over two of the three axes in the molecule, a pronouncedly axial 'inverse' powder EPR spectrum is obtained, showing "$g_\perp$" > "$g_\parallel$" > 2.00.[19,22,45–51] In this case, "$g_\perp$" is equal to the average of the true g_1 and g_2 parameters for the compound, while "$g_\parallel$" (which is not involved in the disorder) is the true g_3 value. If the distribution of the Jahn–Teller axis over the different disorder sites is not equal, then the spectrum will be of lower symmetry, with apparent g-values that are the appropriate weighted averages of the true values. An inverse EPR spectrum from a disordered $\{d_{x^2-y^2}\}^1$ spin can be distinguished from that of a true $\{d_{z^2}\}^1$ site by a higher value of $g_\parallel$ or g_3, which will usually be ≥2.03 for a $\{d_{x^2-y^2}\}^1$ Cu(II) ion but should be ≤2.01 for a $\{d_{z^2}\}^1$ Cu(II) site.[8,9] In addition, a disordered spin will not normally show any resolved EPR hyperfine coupling interactions (Fig. 3); so, an inverse EPR signal with resolved coupling to ^{63,65}Cu must arise from a $\{d_{z^2}\}^1$ complex (Fig. 1).

This behaviour is illustrated by the powder EPR behaviour of the fluxional complex $[Cu(L^2H)_2][BF_4]_2$ (Fig. 2), which shows an axial 'inverse' signal at 290 K ($g_\perp$ = 2.195, $g_\parallel$ = 2.043; Fig. 3).[22] This reflects disorder of a Jahn–Teller axis of elongation over all four of the Cu–N{pyrazole} bonds in the molecule. The spectrum becomes rhombic as the temperature is lowered, causing the axis of Jahn–Teller elongation to become progressively more localised in one of the two disorder orientations.[22] Below 40 K the spectrum becomes more complex, owing to partial freezing out of the Jahn–Teller fluxionality. The spectra at these low temperatures contain distinct signals originating from dynamic and static Cu(II) spins.

On top of these complications, misleading g-values can also be observed in powder EPR spectra if the sample is sufficiently

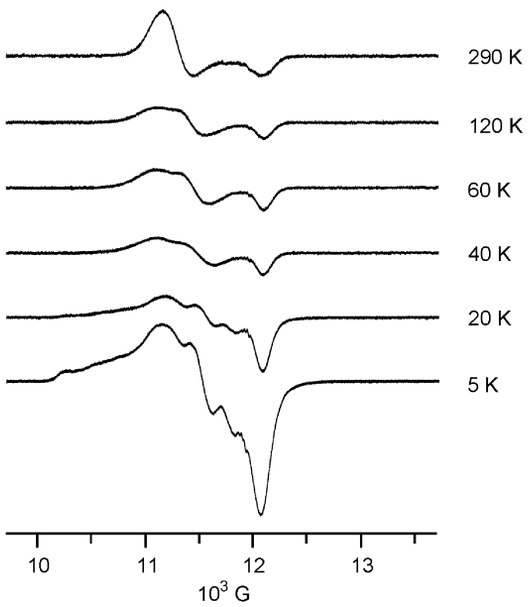

Fig. 3 Variable temperature Q-band powder EPR spectra of $[Cu(L^2H)_2][BF_4]_2$ (Fig. 2).[22]

crystalline that the orientations of spins in the material are not truly random; or, if there are significant dipolar interactions between molecules in the sample.[20] Unless a (time-consuming) single crystal EPR analysis is undertaken, the surest way to obtain the true EPR symmetry of a molecular Cu(II) compound is by running the dissolved sample as a frozen glass.[51–53] Individual molecules in solution have truly random orientations and are well-separated from each other, so that their spectra are uncontaminated by intermolecular interactions or orientational effects. To confirm that the solid state structure of the compound is retained in solution, spectra should be run in different solvents, ideally in conjunction with UV/vis and conductivity measurements under the same conditions. Alternatively, doping the Cu(II) compound of interest into a diamagnetic solid host can also yield EPR spectra with improved resolution.[41,44,54] However, dissolution of the sample into a solvent or a solid host may enforce a different molecular structure onto the Cu(II) sites than in the pure Cu compound (see below).

These methods have been used to assign disordered, Jahn–Teller elongated structures to many Cu(II) compounds with apparently anomalous coordination geometries (see ESI†). In several cases, these compounds were originally mis-assigned as showing "quenched" Jahn–Teller effects or Jahn–Teller compressions, which was subsequently corrected after further study. Before our own work, described below, there were no molecular six-coordinate Cu(II) complexes in which a Jahn–Teller compressed structure had been rigorously demonstrated. However, there are several other known Cu(II) complexes with unusual stereochemistries in the crystal, which have not yet been studied in depth and would benefit from reinvestigation.[55]

Inorganic copper compounds containing compressed six-coordinate Cu(II) centres

The first pure (rather than doped) Cu(II) compound in which a tetragonally compressed molecular structure was unambiguously demonstrated was the inorganic salt $KAlCuF_6$. This compound is not formed from discrete $[CuF_6]^{4-}$ octahedra; rather, it contains 1-D zigzag chains of vertex-sharing, C_2-symmetric *trans*-$[CuF_4(\mu\text{-}F)_2]^{3-}$ centres (Fig. 4).[56] The Cu ions in this structure have distorted octahedral structures that are compressed along the (μ-F)–Cu–(μ-F) vectors, the Cu–F distances being 1.873(3), 1.881(3), 2.122(3) (×2) and 2.124(3) (×2) Å. Superexchange and dipolar interactions between the

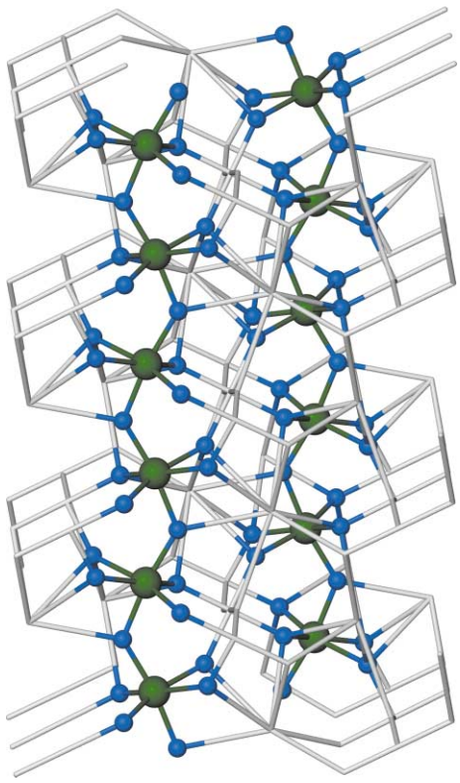

Fig. 4 Partial packing diagram of $KAlCuF_6$,[56] highlighting the chains of vertex-sharing $[CuF_6]^{4-}$ octahedra. The Cu atoms are in green and the F atoms are blue.

covalently linked Cu ions in this structure mean that the EPR properties of the individual Cu(II) spins in $KAlCuF_6$ cannot be probed. However, a combination of single-crystal UV/vis spectroscopy,[18] magnetic susceptibility measurements,[57] angular overlap theoretical calculations[57] and EXAFS measurements[58] unequivocally demonstrated that the crystallographically observed axial compression is a true indication of the molecular structure of the compound. Importantly, all of the large number of other known compounds containing $[CuF_6]^{4-}$ octahedra adopt Jahn–Teller elongated structures, although these are sometimes crystallographically disordered; examples include, but are not limited to, CuF_2,[59] $MCuF_3$ (M = Na,[60] K,[61] Rb[60]), M_2CuF_4 (M = Na,[62] K,[63–65] Tl[66]), $K_3Cu_2F_7$,[66] $NaCu_3F_7$[67] and $CuMF_6$ (M = Mo,[68] Pt,[69] Sn[70]). The 2-D ferromagnet K_2CuF_4 was originally assigned as an axially compressed octahedron as a result of an incorrect space group assignment,[71] which has since been corrected.[63–65]

Jahn–Teller compressed structures have also been claimed in a small number of inorganic Cu(II) oxyanion compounds. Two closely related examples are $Cu_3(OH)_2(V_2O_7)\cdot 2H_2O$ (the mineral volborthite)[72] and $KCu_3(OH)_2(H[AsO_4]_2)$.[73] These structures are both composed of chains of edge-sharing, rhombically elongated $[CuO_6]$ octahedra, which are linked into sheets by additional bridging interactions to apparently tetragonally compressed $[CuO_6]$ centres (Fig. 5). The Cu–O bond lengths to the latter Cu ion in $KCu_3(OH)_2(HAs_2O_8)$ are shown in Scheme 4; the corresponding parameters for volborthite are 1.945(4) (×2) and 2.172(4) (×4) Å. We have carried out a MSDA analysis on $KCu_3(OH)_2(HAs_2O_8)$, and found that $\langle d^2 \rangle$ for all the Cu–O bonds to the compressed Cu centre is ≤18 × 10^{-4} Å^2 (Scheme 4). Hence, while spectroscopic confirmation is lacking, the assignment of a Jahn–Teller compressed configuration in this structure is probably correct. A similar analysis for volborthite is impossible, since anisotropic thermal parameters for this compound were not published.

Reports of compressed octahedral Cu(II) centres in other copper oxyanion structures are less certain. A MSDA analysis of the putative "compressed" Cu site in $Cu_3Cr_4[PO_4]_6$[74]

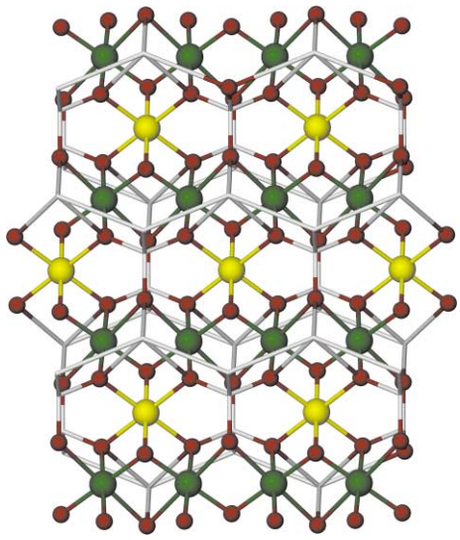

Fig. 5 Partial packing diagram of $KCu_3(OH)_2(H[AsO_4]_2)$, showing the layers of linked [CuO_6] centres.[73] The tetragonally compressed Cu atoms are highlighted in yellow, while the Jahn–Teller-elongated Cu ions are in green and the O atoms are red. The structure of volborthite is composed of layers of [CuO_6] centres with the same topology shown here.

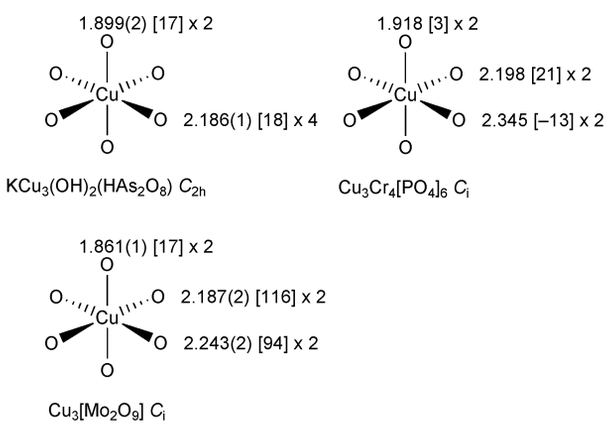

Scheme 4 Bond lengths (Å), and $<d^2>$ values ($\times 10^4$ Å^2) in square brackets, three compounds containing CuO_6 centres, for which pseudo-Jahn–Teller compressed structures have been proposed.[73–75] The crystallographic site symmetry for each of these Cu sites is also given. See text for further details.

(Scheme 4) implies that this is not a disordered Cu centre. However, the highly rhombic distribution of Cu–O bond lengths (Scheme 4) makes it uncertain whether this should be treated as a Jahn–Teller compressed or elongated structure. The EPR spectrum of this compound, which might have clarified this question, is uninformative.[74] The claim of a Jahn–Teller compressed six-coordinate Cu site in $Cu_3[Mo_2O_9]$[75] seems less likely, on the basis of a MSDA analysis (Scheme 4). The higher values of $<d^2>$ for the two longer Cu–O bonds strongly imply that there is unresolved librational disorder along them. The suggestion that γ-$Cu_2(OH)_3Cl$ (paratacamite) contains a tetragonally compressed [CuO_6] site[76] has been undermined, by the demonstration that paratacamite is not a pure copper mineral.[77] Finally, the assignment of a Jahn–Teller compressed structure to a copper oxalate phase, on the basis of its inverse EPR spectrum, seems unlikely given the *g*-values observed for this material of $g_\perp = 2.209$ and $g_\parallel = 2.071$.[78] The very high value of $g_\parallel$ here is much more suggestive of a $\{d_{x^2-y^2}\}^1$ spin, whose orientation in the solid is disordered, or in which the principal axes of adjacent molecules in the lattice are accidentally coincident.

There is also one series of heteroleptic hexacoordinate Cu(II) complexes, where a compressed [2 + 4] coordination geometry is observed. These are β-$CuX_2(NH_3)_2$ (X^- = Cl^- or Br^-), which consist of linear chains of edge-sharing *trans*-[$Cu(\mu\text{-}X)_4(NH_3)_2$] compressed octahedra with D_{2h} site symmetry (Fig. 6).[79] α-[$CuBr_2(NH_3)_2$] also contains chains of D_{2h} edge-sharing *trans*-[$Cu(\mu\text{-}Br)_4(NH_3)_2$] octahedra, but differs from the β-modification in that the Cu centres now have a clear pseudo-Jahn–Teller elongation along one Br–Cu–Br axis (Fig. 6).[80] α-$CuCl_2(NH_3)_2$ is not isomorphous with α-$CuBr_2(NH_3)_2$, and has not been fully characterised.[81] The β-polymorph of both compounds is metastable and converts slowly to the α-form at room temperature; this transformation can be reversed upon application of pressure.[82] The visible and IR spectra[16] and magnetic superexchange interactions[83] shown by α- and β-$CuX_2(NH_3)_2$ (X^- = Cl^- or Br^-) are notably different, which would not be the case if β-$CuX_2(NH_3)_2$ were simply equivalent to the α-form, but with an elongation axis disordered over the two Br–Cu–Br vectors. Hence, β-$CuX_2(NH_3)_2$ contains genuinely tetragonally compressed Cu(II) centres. In fact, the Cu $d_{x^2-y^2}$ and d_{z^2} orbitals in β-$CuBr_2(NH_3)_2$ are separated by <1 cm^{-1} according to angular overlap calculations.[84] This makes β-$CuBr_2(NH_3)_2$ close to a true example of a quenched (pseudo)-Jahn–Teller effect. The α- and β-structures of $CuX_2(NH_3)_2$ are sometimes referred to as 'distortion isomers'.[85]

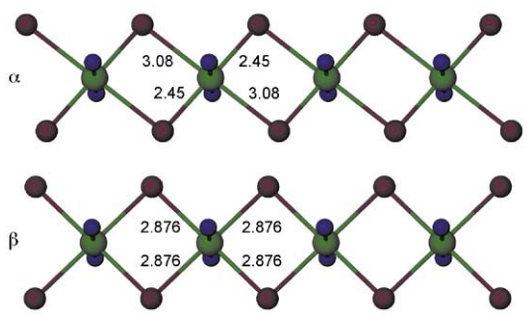

Fig. 6 Structures of the complex chains in α- and β-[$CuBr_2(NH_3)_2$],[79,80] showing the Cu–Br bond lengths in the two structures. The Cu–N distances are 1.93 (×2, α) and 2.034 (×2, β) Å. The Cu ions are green, N blue and Br maroon. H atoms were not included in either structure determination. The host compounds $HgCl_2(NH_3)_2$[96] and $CdCl_2(pz)_2$[97] are 1-D chain structures with the same basic topology shown here.

The salt $[Et_3NH]_2CuCl_4$ contains 2-D layers of corner-sharing *trans*-$[CuCl_2(\mu\text{-}Cl)_4]^{2-}$ octahedra.[86] The axis of Jahn–Teller elongation at these centres is crystallographically ordered within these layers (Fig. 7), with a very long axial Cu ··· Cl distance of 2.975(5) Å. Application of *ca.* 4 GPa of hydrostatic pressure to this material causes disappearance of the Raman-active ν_{Cu-Cl} vibrations, and substantial red-shifting of its Cl ⟶

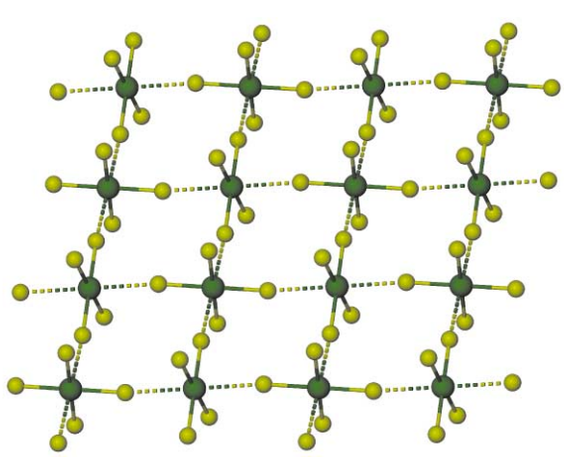

Fig. 7 Partial structure of one 2-D layer in the structure of $[Et_3NH]_2CuCl_4$.[86] The Et_3NH^+ ions have been omitted for clarity. The Cu atoms are in green, the Cl atoms are in yellow and the Jahn–Teller elongated Cu–Cl bonds are shown as dotted lines.

Cu charge-transfer spectrum.[87] These data were interpreted as showing the disappearance of the in-plane Jahn–Teller distortion of the Cu sites under pressure, yielding a material with a quenched Jahn–Teller distortion similar to that in β-$CuX_2(NH_3)_2$ (see above). Similar results have been obtained from pressurised, isostructural Cu-doped $[R_3NH]_2MCl_4$ (R = alkyl, M = Mn or Cd) hosts.[88,89] Interestingly, the Cu sites in $[ND_4]_2[Cu(OD_2)_6][SO_4]_2$ react to pressure in a different way. They retain a Jahn–Teller elongated configuration; but, this structural elongation rotates from one O–Cu–O axis of the $[Cu(OD_2)_6]^{2+}$ octahedron to another as the pressure is increased.[90]

Host lattices that enforce a compressed octahedral structure onto doped Cu(II) ions

A small number of Cu(II)-doped solids are also known, in which a Jahn–Teller compression is enforced onto the copper sites by the constraints of the surrounding lattice. One example is Cu-doped NH_4X (X^- = Cl^-, Br^-), which contains well-separated Cu(II) centres that are crystallographically very similar to the individual Cu ions in β-$CuX_2(NH_3)_2$ (see above).[91] With sufficiently low doping levels, well-resolved axial EPR spectra can can be obtained that are not significantly temperature-dependent, and show $g_\perp = 2.20(2)$ and $g_\parallel = 2.01(1)$ with resolved hyperfine coupling on both components of the spectra.[92,93] These spectra are clearly consistent with the crystallographically observed [2 + 4] distribution of Cu–ligand bond lengths. Similar EPR and visible spectra were obtained for $Cu_zHg_{1-z}X_2(NH_3)_2$ (X^- = Cl^-, Br^-; $z \leq 0.05$)[92,94] and $Cu_{0.02}Cd_{0.98}Cl_2(pz)_2$ (pz = pyrazole).[95] The pure compounds $HgCl_2(NH_3)_2$ and $CdCl_2(pz)_2$ both have structures composed of 1-D chains of edge-sharing *trans*-$[M(\mu\text{-}Cl)_4L_2]$ (M = Hg, L = NH_3;[96] M = Cd, L = pz[97]) octahedra whose local coordination geometries are very similar to those in β-$CuX_2(NH_3)_2$ (Fig. 6). Hence it is reasonable that Cu ions doped into these structures, and into NH_4Cl, should closely resemble one another.

Another well-studied example is $K_2Cu_zZn_{1-z}F_4$. The host lattice K_2ZnF_4 contains of 2-D layers of corner-sharing *trans*-$[ZnF_2(\mu\text{-}F)_4]^{2-}$ octahedra with a similar, but more regular, topology to that in $[Et_3NH]_2CuCl_4$ (Figs. 7, 8).[98] The Zn centres in this material have D_{4h} site symmetry with six effectively equal Zn–F bond lengths.[98] The doped material $K_2Cu_zZn_{1-z}F_4$ with low Cu concentrations (z <0.1) shows an axial EPR spectrum that clearly demonstrates a $\{d_{z^2}\}^1$ structure, with $g_\perp = 2.39(1)$ and $g_\parallel = 2.01(1)$.[65,99] Presumably, the two terminal F^- ligands

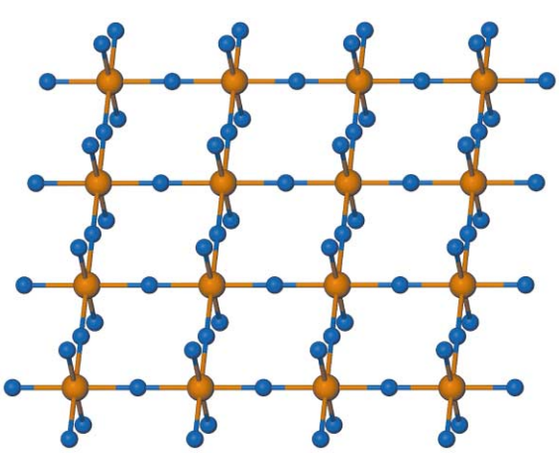

Fig. 8 Partial structure of one 2-D layer in K_2ZnF_4.[98] The K^+ ions have been omitted for clarity. The Zn atoms are in orange, and the F atoms in blue. K_2CuF_4 is isomorphous, with a Jahn–Teller elongation that is statically disordered over the two (μ-F)–Cu–(μ-F) axes on each metal centre (*cf.* Fig. 7). The host lattice Ba_2ZnF_6 also contains 2-D layers of $[ZnF_4]^{2-}$ centres with an identical topology to the one shown.

are stronger donors than the four bridging F^-, thus affording an axially compressed structure.[65] Although the shape of the EPR spectrum does not vary at higher Cu concentrations, its linewidth and angular dependence (in the single crystal) does change in a way consistent with the onset of chemical exchange. Hence, when z >0.1 the Cu centres adopt a fluxional $\{d_{x^2-y^2}\}^1$, pseudo-Jahn–Teller elongated structure that, for z >0.45, becomes statically disordered in a manner identical to that in pure K_2CuF_4.[65] Consistent with this, the d–d absorptions shown by $K_2Cu_zZn_{1-z}F_4$ also vary with increasing z, showing that the structure of the Cu sites in the material changes as the Cu concentration increases.[65] Similar results were found in Cu-doped Ba_2ZnF_6,[100] which contains 2-D layers of corner-sharing *trans*-$[ZnF_2(\mu\text{-}F)_4]^{2-}$ octahedra like those in K_2ZnF_4, but with a more pronounced axial compression at the Zn centres.[101] In $Ba_2Cu_zZn_{1-z}F_6$, the transition from an axially compressed geometry at Cu to a disordered, rhombically elongated one occurs for $z \approx 0.6$.[100] These results reflect a competition between the natural axial compression present in the metal site of the host lattice; and, the tendency of six-coordinate Cu(II) to adopt an elongated geometry. At higher Cu concentrations, the structural preference of the Cu ions becomes dominant and causes the structural switch. The Cu(II) ions forming adjacent Cu : Mn pairs in $KCu_{0.015}Mn_{0.015}Zn_{0.97}F_3$ have an axially compressed structure,[102] even though the isolated Cu centres in $KCu_zZn_{1-z}F_3$ are more normal elongated octahedra.[103] The origin of this effect is uncertain.

The alkaline earth oxides have the rock salt structure, with cubic site symmetry at both the metal and oxide ions. Isolated Cu(II) ions doped into MgO and CaO show EPR spectra that are apparently isotropic until very low temperatures, and which show only small g-splittings even at 1.2 K.[104] These data have been interpreted on the basis of Cu sites showing unusually small Jahn–Teller distortions, which are dynamically disordered over all three axes of the cubic unit cell. Interestingly, the low-temperature configuration of Cu(II) ions in MgO is $\{d_{x^2-y^2}\}^1$, while in CaO it is $\{d_{z^2}\}^1$.[104,105] This difference may be related to the ionic radii of the host and doped cations, which follows the ordering $Mg^{2+} \approx Cu^{2+} < Ca^{2+}$.[106] A compressed octahedral structure, where four of the six Cu–O bonds are long, allows the smaller Cu(II) ion to be better accommodated within the Ca sites of the host material.[14] Interestingly, adjacent ferromagnetically coupled Cu–O–Cu pairs doped into CaO exhibit different configurations by EPR, with one Cu ion per pair being $\{d_{x^2-y^2}\}^1$ and one $\{d_{z^2}\}^1$.[107]

Other doped oxo or oxyanion lattices that contain a compressed six-coordinate Cu(II) environment by EPR include $Mg_{1-z}Cu_{2+z}O_3$ (z = 0.1),[108] Pb(Zn,Cu)(OH)(VO_4) (the mineral descloizite),[109] $[NH_4]_2[Cu_zZn_{1-z}(NH_3)_2(CrO_4)_2]$ (z = 0.005)[110] and Cu(II) doped into $Na_2HAsO_4{\cdot}7H_2O$.[111]

Control of the d-orbital configuration in some molecular Cu(II) complexes

Our own interest in this area began when we started to investigate the chemistry of 2,6-di(pyrazol-1-yl)pyridine ligands (L^2R). We had found that $[Cu(L^2H)_2][BF_4]_2$ has a fluxional pseudo-Jahn–Teller elongated structure in the solid (Fig. 2),[22,25,33,52] and reasoned that this fluxionality could be prevented in other $[Cu(L^2R)_2]^{2+}$ complexes if the 'R' substituents were sufficiently large. In that case, steric repulsion between the 'R' substituents of one coordinated ligand, and the pyridyl backbone of the other, should enforce an axially compressed structure along the N{pyridine}–Cu–N{pyridine} direction (Scheme 5). This approach was successful, in that $[Cu(L^2Ph)_2][BF_4]_2$[112] and $[Cu(L^2Mes)_2][BF_4]_2$ (Fig. 9)[21,52] both exhibited clearly resolved axial or rhombic EPR spectra with $g_1 \geq g_2 > g_3 \approx 2.00$ in the solid state *and* in solution, that are essentially temperature-independent (Table 1). All these spectra have observable ^{63,65}Cu hyperfine coupling, on at least the g_3

Table 1 Q-band EPR data for six-coordinate Cu(II) complexes with a $\{d_{z^2}\}^1$ ground state. Related $\{d_{y^2-z^2}\}^1$ compounds are also listed for the purposes of comparison. Hyperfine couplings are to ^{63,65}Cu and are in G. Unless otherwise stated, the estimated errors on these parameters are $g \pm 0.002$, $A \pm 2$ G

	Ground state	Phase	T/K	g_1	g_2	g_3	A_1	A_2	A_3	Ref.
$[Cu(L^2H)_2][BF_4]_2$	$\{d_{y^2-z^2}\}^1$	Powder[a]	5	2.32(4)	2.093	2.042	200(50)	–	–	22
		MeCN	120	2.281	2.099	2.051	137	–	–	22
$[Cu(L^2Ph)_2][BF_4]_2$	$\{d_{z^2}\}^1$	Powder	115	2.235	2.210	2.007	115	–	134	112
		MeCN	115	2.235	2.175	2.015	115	–	140	112
$[Cu(L^2Mes)_2][ClO_4]_2$	$\{d_{z^2}\}^1$	Powder	115	2.248	2.145	2.015	105	–	100	52
		MeCN[b]	115	2.200	2.200	2.007	75	75	104	52
α-$[Cu(L^3)_2][ClO_4]_2$	$\{d_{y^2-z^2}\}^1$	Powder[a]	5	2.300	2.087	2.057	135	–	–	51
		MeCN	120	2.281	2.099	2.051	137	–	–	51
$[Cu(L^1Cy)_2][BF_4]_2$	$\{d_{y^2-z^2}\}^1$	Powder[c]	10	2.256	2.073	2.040	154	–	–	53
		MeCN	110	2.252	2.081	2.042	144	–	–	53
$[Cu(L^1tBu)_2][BF_4]_2$	$\{d_{z^2}\}^1$	Powder[b,c]	10	2.219	2.219	1.998	–	–	161	53
		MeCN	110	2.220	2.215	2.001	–	–	165	53
$[Cu(L^1NH_2)_2][ClO_4]_2$	$\{d_{z^2}\}^1$	Powder	295	2.198	2.169	2.014	–	–	91	117
	$\{d_{y^2-z^2}\}^1$	Powder	5	2.252	2.097	2.034	–	–	–	117
$[Cu(L^1OH)_2][ClO_4]_2$	$\{d_{z^2}\}^1$	Powder	295	2.207	2.177	2.012	–	–	–	117
$[Cu(L^4)_2][ClO_4]_2$	$\{d_{z^2}\}^1$	Powder[b]	10	2.221	2.221	2.001	–	–	170	53

[a] This EPR spectrum contains distinct signals arising from fluxional and static Cu(II) centres. Only the static EPR parameters are quoted. [b] This spectrum has axial symmetry. [c] See Fig. 1.

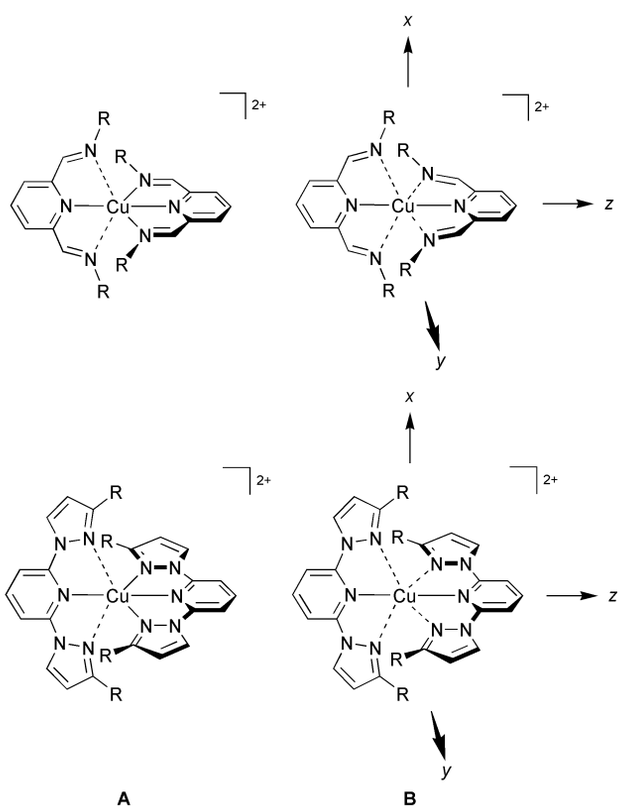

Scheme 5 Comparative molecular structures of $[Cu(L^1R)_2]^{2+}$ and $[Cu(L^2R)_2]^{2+}$ complexes with the ground states: (**A**) $\{d_{y^2-z^2}\}^1$;‡ or (**B**) $\{d_{z^2}\}^1$.[4] The solid and dotted Cu–N bonds are short and long, respectively. The molecular axes of the molecules used to derive these ground state labels are also shown.

component. These data clearly indicate that these compounds adopt a $\{d_{z^2}\}^1$ ground state, and hence the desired axially compressed structure. The bulkier ligands L^2tBu[113] and L^2CF_3[114] did not yield isolable $[Cu(L^2R)_2]^{2+}$ (R = *t*Bu, CF_3) complexes, presumably for steric reasons.

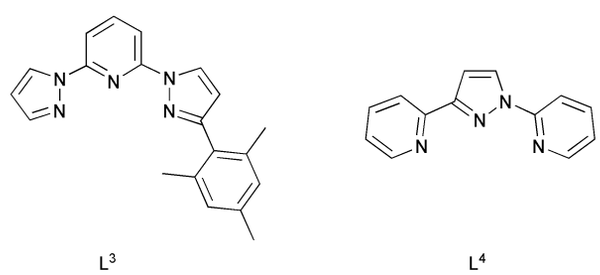

In order to obtain a true structural comparison between $[Cu(L^2R)_2]^{2+}$ centres with $\{d_{y^2-z^2}\}^1$ and $\{d_{z^2}\}^1$ ground states,‡ we had to obtain crystal structures at 30 K where the Jahn–Teller fluxionality shown by $[Cu(L^2H)_2][BF_4]_2$ is frozen out.[22,33] This compound, and $[Cu(L^2Mes)_2][ClO_4]_2$, both show rhombic coordination geometries at this temperature (Figs. 2 and 9), the change in d-orbital occupancy having quite subtle effects on their Cu–N bond lengths (Table 2).[51] The two sets of Cu–N{pyrazole} bond lengths near the molecular *x*- and *y*-axes (Scheme 5), have converged in $[Cu(L^2Mes)_2]^{2+}$ compared to $[Cu(L^2H)_2]^{2+}$, by between 0.043(3) and 0.076(3) Å. Interestingly, however, there is a much smaller *z*-axis contraction in the $\{d_{z^2}\}^1$ complex, of 0.023(3)–0.031(3) Å. For these reasons, we prefer to describe the structural distortion in $[Cu(L^2Mes)_2]^{2+}$ as an elongation of the Cu–N bonds within the *xy* ligand plane, rather than as a *z*-axis compression.

We can be confident that the molecular structure of $[Cu(L^2Mes)_2]^{2+}$ reflects the preferences of the $\{d_{z^2}\}^1$ Cu(II) ion, rather than the steric properties of the L^2Mes ligand, for two reasons. First, the mono-substituted ligand complex $[Cu(L^3)_2][ClO_4]_2$ exhibits a $\{d_{y^2-z^2}\}^1$ configuration,‡ with static Cu–N bond lengths that are similar to those of $[Cu(L^2H)_2][BF_4]_2$ (Tables 1

‡ Strictly speaking, the electronic configuration of $[Cu(L^2H)_2]^{2+}$, $[Cu(L^1Cy)_2]^{2+}$ and related compounds is $\{d_{y^2-z^2}\}^1$ rather than $\{d_{x^2-y^2}\}^1$, because the axis of structural elongation does not lie on what would be the unique molecular axis by symmetry, in the absence of the pseudo-Jahn–Teller distortion. Hence, the pseudo-Jahn–Teller elongation lies along the *x*- rather than the *z*-axis of the molecule (Scheme 5).

Table 2 Cu–N bond lengths (Å) in six-coordinate Cu(II) complexes with a $\{d_{z^2}\}^1$ ground state. Related $\{d_{x^2-y^2}\}^1$ compounds are also listed for the purposes of comparison. See Scheme 5 for the molecular axis convention used in this Table

			Cu–N bond lengths aligned close to the molecular:			
	T/K	Ground state	*x*-axis	*y*-axis	*z*-axis	Ref.
$[Cu(L^2H)_2][BF_4]_2$:	31					33
molecule A		$\{d_{x^2-y^2}\}^1$	2.282(2), 2.290(2)	2.056(2), 2.076(2)	1.967(2), 2.028(2)	
molecule B		$\{d_{x^2-y^2}\}^1$	2.261(2), 2.286(2)	2.072(2), 2.088(2)	1.963(2), 2.037(2)	
molecule C		$\{d_{x^2-y^2}\}^1$	2.266(2), 2.306(2)	2.056(2), 2.077(2)	1.958(2), 2.026(2)	
α-$[Cu(L^3)_2][ClO_4]_2\cdot 2CH_3NO_2$	30	$\{d_{x^2-y^2}\}^1$	2.2741(14), 2.3048(13)	2.0928(14), 2.1012(14)	1.9668(14), 2.0343(14)	51
$[Cu(L^2Mes)_2][ClO_4]_2\cdot 2CH_3NO_2$	31	$\{d_{z^2}\}^1$	2.2117(15), 2.2503(15)	2.1371(14), 2.1463(14)	1.9586(14), 1.9799(14)	51
$[Cu(L^1Cy)_2][BF_4]_2\cdot CH_3NO_2$	150	$\{d_{x^2-y^2}\}^1$	2.412(2), 2.443(2)	2.085(2), 2.091(2)	1.936(2), 2.004(2)	53
$[Cu(L^1tBu)_2][BF_4]_2\cdot ½(CH_3)_2CO$:	150					
molecule A		$\{d_{z^2}\}^1$	2.312(2), 2.450(2)	2.295(2), 2.304(2)	1.932(2), 1.958(2)	53
molecule B		$\{d_{z^2}\}^1$	2.349(2), 2.352(2)	2.278(2), 2.313(2)	1.927(2), 1.934(2)	
$[Cu(L^1OH)_2][ClO_4]_2\cdot 2(CH_3)_2CO$	300	$\{d_{z^2}\}^1$	2.285(3), 2.295(3)	2.205(3), 2.211(3)	1.933(3), 1.958(3)	117
$[Cu(L^4)_2][ClO_4]_2$	293	$\{d_{z^2}\}^1$	2.233(9), 2.353(9)	2.297(8), 2.326(8)	1.824(8), 1.838(9)	53

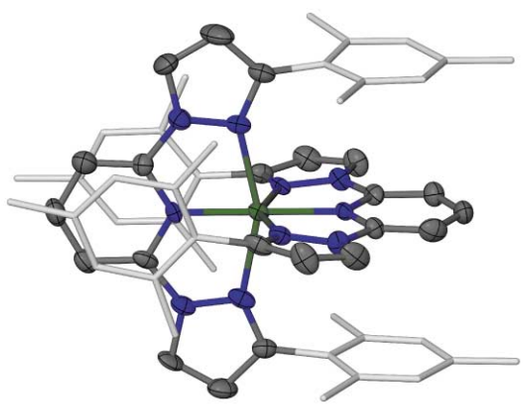

Fig. 9 View of the $\{d_{z^2}\}^1$ complex dication in the crystal structure of $[Cu(L^2Mes)_2][ClO_4]_2\cdot 2CH_3NO_2$ (Table 2) at 180 K.[52] All H atoms have been omitted for clarity. Colour code: C = grey or white, N = blue, Cu = green.

and 2).[51] This includes a bond of 2.1012(14) Å, between the Cu ion and a 3-mesitylpyrazolyl donor. Second, low-spin $[Fe(L^2Mes)_2][PF_6]_2$ shows six extremely short Fe–N bond lengths, of 1.8936(18)–2.0049(18) Å.[115] Both these results imply that that the L^2Mes ligand could support much shorter Cu–N{pyrazole} bonds than are observed in $[Cu(L^2Mes)_2][ClO_4]_2$. Hence, the structural differences between $[Cu(L^2H)_2]^{2+}$ and $[Cu(L^2Mes)_2]^{2+}$ are not sterically imposed.

We explored the generality of this phenomenon, using $[Cu(L^1R)_2][BF_4]_2$.[53] Similar results were obtained from this system, although a larger ligand 'R' substituent was required to enforce the change in electronic structure. Hence, solid $[Cu(L^1Cy)_2][BF_4]_2$ shows a static $\{d_{x^2-y^2}\}^1$ ground state by EPR and X-ray crystallography, ‡ while $[Cu(L^1tBu)_2][BF_4]_2$ is a $\{d_{z^2}\}^1$ species (Fig. 1, Table 1).[53] Comparison of the crystal structures of the two complexes showed the same trends as for the $[Cu(L^2R)_2]^{2+}$ system (Table 2). However, the differences between the Cu–N distances in the $[Cu(L^1R)_2]^{2+}$ compounds are more pronounced, reflecting the greater flexibility of the L^1R ligand backbone.

We have also produced six-coordinate $\{d_{z^2}\}^1$ Cu(II) complexes using other methods of perturbing the Cu centre. First, $[Cu(L^4)_2][ClO_4]_2$ shows a clear structural compression, with very long Cu–pyridine bonds (Tables 1 and 2).[53] This is a reflection of the narrower internal angles of the central pyrazole ring in L^4, compared to the pyridine ring in L^2R, which prevent the pyridine donors from approaching the Cu ion more closely.[116] So, the $\{d_{z^2}\}^1$ configuration in $[Cu(L^4)_2]^{2+}$ is induced by conformational strain within the ligand backbone, rather that by inter-ligand steric repulsion. Finally, the hydrazone and oxime ligand complexes $[Cu(L^1NH_2)_2][ClO_4]_2$ and $[Cu(L^1OH)_2][ClO_4]_2$ (Scheme 3) also adopt a $\{d_{z^2}\}^1$ configuration at room temperature by powder EPR and by crystallography (Tables 1 and 2).[117] Intriguingly, these EPR spectra are temperature-dependent. For $[Cu(L^1NH_2)_2][ClO_4]_2$, at least, the spectra strongly imply that the complex transforms from a $\{d_{z^2}\}^1$ species at room temperature, to a $\{d_{x^2-y^2}\}^1$ configuration at 5 K. Although the spectra of $[Cu(L^1OH)_2][ClO_4]_2$ are contaminated by intermolecular effects, the crystal structure of a solvate of this complex is also temperature-dependent, in a manner consistent with the EPR data. Importantly, a MSDA analysis of the Cu–N bond lengths shows that librational disorder is *not* present. Hence, these two compounds appear to exhibit the unique property, of having a temperature-dependent Jahn–Teller distortion. Since $[Cu(L^1R)_2][BF_4]_2$ (R = Me, Cy) are $\{d_{x^2-y^2}\}^1$ complexes,[53] the ground state of $[Cu(L^1R)_2]^{2+}$ therefore depends on the inductive, as well as the steric, properties of the ligand imine donors.

Concluding remarks

The natural tendency of six-coordinate Cu(II) to adopt a Jahn–Teller elongated stereochemistry has been circumvented in a small, but very diverse, group of compounds. In pure or doped inorganic solids, the steric constraints of a surrounding lattice will sometimes impose a Jahn–Teller compressed octahedral structure onto a Cu(II) centre. In one structure, namely β-$CuX_2(NH_3)_2$, similar considerations lead to an undistorted structure in which the (pseudo)-Jahn–Teller effect has been effectively quenched. However, this phase is only metastable at room temperature; the Jahn–Teller effect still wins in the end.

The only molecular six-coordinate Cu(II) compounds, in which a $\{d_{z^2}\}^1$ ground state has been confirmed by in-depth characterisation, are of the type $[CuL_2]^{2+}$ where 'L' is a linear *tris*-N-donor ligand. In this geometry, a structural compression along the unique molecular axis (*z* in Scheme 5) can be enforced using sterically bulky or electron-withdrawing substituents, or a conformationally constrained ligand, to weaken the four distal Cu–N bonds. This is *not* a Jahn–Teller compression, since the *z*-axis is not degenerate in the idealised D_{2d} symmetry shown by these compounds in the absence of Jahn–Teller effects. Rather, the rhombic stereochemistries adopted by $[Cu(L^1R)_2]^{2+}$ (R = *t*Bu, NH_2 or OH), $[Cu(L^2R)_2]^{2+}$ (R = Ph or Mes) and $[Cu(L^4)_2]^{2+}$ represent partially quenched pseudo-Jahn–Teller

distortions, comparable to the fully quenched distortion in β-$CuX_2(NH_3)_2$. Several other octahedral Cu(II) complexes also apparently show compressed or quenched Jahn–Teller distortions by crystallography or EPR. However, in every case that has been properly studied this has been shown to be an artifact, caused by disorder of a Jahn–Teller elongation (see ESI†). The same issues also apply to octahedral compounds of other Jahn–Teller ions, notably high-spin Cr(II) and Mn(III) and low-spin Co(II).[15]

Since we can control the Jahn–Teller effect in these Cu(II) complexes, the next question is whether or not it might be *switched*. The inductive control of ground state shown by $[Cu(L^1R)_2]^{2+}$ does hold out that possibility, in that sterically small, protonatable or oxidisable 'R' substituents could be used to control the basicity of a ligand's distal N donors. Protonation or oxidation of that substituent in a $\{d_{y^2-z^2}\}^1$ Cu(II) complex would make it more electron-withdrawing, thus weakening the distal Cu–N bonds and potentially causing the metal ion to flip to a $\{d_{z^2}\}^1$ configuration. This represents an interesting challenge for ligand design, that we are enthusiastically tackling.

Acknowledgements

Much of our work described here was carried out by Dr Nayan Solanki and Joanne Holland, with the assistance of Drs Frank Mabbs and Eric McInnes (University of Manchester), Dr Adam Bridgeman (University of Hull), Professor Mary McPartlin (University of North London) and Professor Judith Howard (University of Durham). The structural database searches in the opening paragraph were carried out using the UK Chemical Database Service.[118] Our work was funded by the EPSRC, the Royal Society (London) and the University of Leeds.

References

1 A. Belsky, M. Hellenbrandt, V. L. Karen and P. Lukusch, *Acta Crystallogr., Sect. B*, 2002, **58**, 364.
2 F. H. Allen, *Acta Crystallogr., Sect. B*, 2002, **58**, 380.
3 J. J. R. Fraústo da Silva and R. J. P. Williams, *The Biological Chemistry of the Elements*, Oxford University Press, Oxford, 2nd edn., 2001, ch. 15, pp. 418–432.
4 C. J. Anderson and M. J. Welch, *Chem. Rev.*, 1999, **99**, 2219; B. Sarkar, *Chem. Rev.*, 1999, **99**, 2535.
5 J. Szymanowski, *Hydroxyoximes and Copper Hydrometallurgy*, CRC Press, Boca Raton, FL, 1993.
6 M. T. Weller and C. S. Knee, *J. Mater. Chem.*, 2001, **11**, 701.
7 A. B. P. Lever, *Inorganic Electronic Spectroscopy*, Elsevier, Amsterdam, 2nd edn., 1984, ch. 6, pp. 554–572.
8 B. A. Goodman and J. B. Raynor, *Adv. Inorg. Chem.*, 1970, **13**, 135; B. J. Hathaway, *Coord. Chem. Rev.*, 1970, **5**, 143.
9 B. J. Hathaway, *Struct. Bonding (Berlin)*, 1984, **57**, 55.
10 I. B. Bersuker, *Coord. Chem. Rev.*, 1975, **14**, 357.
11 H. Yamatera, *Acta Chem. Scand., Ser. A*, 1979, **33**, 107.
12 C. J. Simmons, *New J. Chem.*, 1993, **17**, 77.
13 B. J. Hathaway, in *Comprehensive Coordination Chemistry*, ed. G. Wilkinson, R. D. Gillard and J. A. McCleverty, Pergamon, Oxford, 1987, vol. 5, ch. 53, pp. 690–711.
14 M. A. Hitchman, *Comments Inorg. Chem.*, 1994, **15**, 197.
15 L. R. Falvello, *J. Chem. Soc., Dalton Trans.*, 1997, 4463.
16 R. J. H. Clark and C. S. Williams, *J. Chem. Soc. A*, 1966, 1425.
17 B. J. Hathaway, M. J. Bew and D. E. Billing, *J. Chem. Soc. A*, 1970, 1090.
18 K. Finnie, L. Dubicki, E. R. Krausz and M. J. Riley, *Inorg. Chem*, 1990, **29**, 3908.
19 H. Stratemeier, B. Wagner, E. R. Krausz, R. Linder, H.-H. Shmidtke, J. Pebler, W. E. Hatfield, L. ten Haar, D. Reinen and M. A. Hitchman, *Inorg. Chem.*, 1994, **33**, 2320.
20 F. E. Mabbs and D. Collison, *Electron Paramagnetic Resonance of d Transition Metal Compounds*, Elsevier, Amsterdam, 1992.
21 A. J. Bridgeman, M. A. Halcrow, M. Jones, E. Krausz and N. K. Solanki, *Chem. Phys. Lett.*, 1999, **314**, 176.
22 N. K. Solanki, M. A. Leech, E. J. L. McInnes, F. E. Mabbs, J. A. K. Howard, C. A. Kilner, J. M. Rawson and M. A. Halcrow, *J. Chem. Soc., Dalton Trans.*, 2002, 1295.
23 B. L. Silver and D. Getz, *J. Chem. Phys.*, 1974, **61**, 638.
24 C. J. Simmons, B. J. Hathaway, K. Amornjarusiri, B. D. Santarsiero and A. Clearfield, *J. Am. Chem. Soc.*, 1987, **109**, 1947.
25 G. S. Beddard, M. A. Halcrow, M. A. Hitchman, M. P. de Miranda, C. J. Simmons and H. Stratemeier, *Dalton Trans.*, 2003, 1028.
26 J. Bebendorf, H.-B. Bürgi, E. Gamp, M. A. Hitchman, A. Murphy, D. Reinen, M. J. Riley and H. Stratemeier, *Inorg. Chem.*, 1996, **35**, 7419.
27 M. A. Hitchman, W. Maaskant, J. van der Plas, C. J. Simmons and H. Stratemeier, *J. Am. Chem. Soc.*, 1999, **121**, 1488.
28 M. J. Riley, M. A. Hitchman and A. W. Mohammed, *J. Chem. Phys.*, 1987, **87**, 3766.
29 J. D. Dunitz, V. Schomaker and K. N. Trueblood, *J. Phys. Chem.*, 1988, **92**, 856.
30 A. L. Spek, PLATON, A multipurpose crystallographic tool, Utrecht University, Utrecht, the Netherlands, 2003.
31 PLATON and WINGX for Windows are both currently available through the Chemical Crystallography website at the University of Glasgow, UK: http://www.chem.gla.ac.uk/~louis/software.
32 L. J. Farrugia, *J. Appl. Crystallogr.*, 1999, **32**, 837.
33 M. A. Leech, N. K. Solanki, M. A. Halcrow, J. A. K. Howard and S. Dahaoui, *Chem. Commun.*, 1999, 2245.
34 M. A. Newton, A. J. Dent and J. Evans, *Chem. Soc. Rev.*, 2002, **31**, 83.
35 P. J. Ellis, H. C. Freeman, M. A. Hitchman, D. Reinen and B. Wagner, *Inorg. Chem.*, 1994, **33**, 1249.
36 T. Astley, P. J. Ellis, H. C. Freeman, M. A. Hitchman, F. R. Keene and E. R. T. Tiekink, *J. Chem. Soc., Dalton Trans.*, 1995, 595.
37 F. Villain, M. Verdaguer and Y. Dromzee, *J. Phys. IV*, 1997, **7**, 659.
38 V. M. Masters, M. J. Riley, M. A. Hitchman and C. Simmons, *Inorg. Chem.*, 2001, **40**, 4478.
39 J. S. Wood, C. P. Keijzers, E. de Boer and A. Buttafava, *Inorg. Chem.*, 1980, **19**, 2213.
40 D. Reinen and S. Krause, *Solid State Commun.*, 1979, **29**, 691.
41 P. V. Bernhardt, R. Bramley, L. M. Engelhardt, J. M. Harrowfield, D. C. R. Hockless, B. R. Korybut-Daszkiewicz, E. R. Krausz, T. Morgan, A. M. Sargeson, B. W. Skelton and A. H. White, *Inorg. Chem.*, 1995, **34**, 3589.
42 I. Bertini, D. Gatteschi and A. Scozzafava, *Inorg. Chim. Acta*, 1974, **11**, L17; I. Bertini, D. Gatteschi and A. Scozzafava, *Inorg. Chem.*, 1977, **26**, 1973.
43 J. H. Ammeter, H. B. Bürgi, E. Gamp, V. Meyer-Sandrin and W. P. Jensen, *Inorg. Chem.*, 1979, **18**, 733.
44 R. S. Glass, L. K. Steffen, D. D. Swanson, G. S. Wilson, R. de Gelder, R. A. G. de Graaf and J. Reedijk, *Inorg. Chim. Acta*, 1993, **207**, 241.
45 T. Astley, H. Headlam, M. A. Hitchman, F. R. Keene, J. Pilbrow, H. Stratemeier, E. R. T. Tiekink and Y. C. Zhong, *J. Chem. Soc., Dalton Trans.*, 1995, 3809.
46 G. F. Kokoszka, J. Baranowski, C. Goldstein, J. Orsini, A. D. Mighell, V. I. Himes and A. R. Siedle, *J. Am. Chem. Soc.*, 1983, **105**, 5627.
47 P. Chaudhuri, K. Oder, K. Wieghardt, J. Weiss, J. Reedijk, W. Hinricht, J. Wood, A. Ozarowski, H. Stratemeier and D. Reinen, *Inorg. Chem.*, 1986, **25**, 2951.
48 J.-V. Folgado, W. Henke, R. Allmann, H. Stratemeier, D. Beltrán-Porter, T. Rojo and D. Reinen, *Inorg. Chem.*, 1990, **29**, 2035.
49 W. Henke and D. Reinen, *Z. Anorg. Allg. Chem.*, 1977, **436**, 187.
50 C. Friebel, *Z. Anorg. Allg. Chem.*, 1975, **417**, 197.
51 N. K. Solanki, M. A. Leech, E. J. L. McInnes, J. P. Zhao, F. E. Mabbs, N. Feeder, J. A. K. Howard, J. E. Davies, J. M. Rawson and M. A. Halcrow, *J. Chem. Soc., Dalton Trans.*, 2001, 2083.
52 N. K. Solanki, E. J. L. McInnes, F. E. Mabbs, S. Radojevic, M. McPartlin, N. Feeder, J. E. Davies and M. A. Halcrow, *Angew. Chem., Int. Ed.*, 1998, **37**, 2221.
53 J. M. Holland, X. Liu, J. P. Zhao, F. E. Mabbs, C. A. Kilner, M. Thornton-Pett and M. A. Halcrow, *J. Chem. Soc., Dalton Trans.*, 2000, 3316.
54 See *e.g.*, R. S. Glass, L. K. Steffen, D. D. Swanson, G. S. Wilson, R. de Gelder, R. A. G. de Graaf and J. Reedijk, *Inorg. Chim. Acta*, 1993, **207**, 241; B. Wagner, S. A. Warda, M. A. Hitchman and D. Reinen, *Inorg. Chem.*, 1996, **35**, 3967.
55 See *e.g.*, U. Turpeinen, R. Hämäläinen and J. Reedijk, *Inorg. Chim. Acta*, 1987, **134**, 87; E. Cole, D. Parker, G. Ferguson, J. F. Gallagher and B. Kaitner, *J. Chem. Soc., Chem. Commun.*, 1991, 1473; A. L. Abuhijleh, J. Pollitte and C. Woods, *Inorg. Chim. Acta*, 1994, **215**, 131; G. De Munno, M. Julve, F. Lloret, J. Cano and A. Caneschi, *Inorg. Chem.*, 1995, **34**, 2048; J. Sletten and O. Bjorsvik, *Acta Chem. Scand.*, 1998, **52**, 770; M. Mimura, T. Matsuo,

Y. Motoda, N. Matsumoto, T. Nakashima and M. Kojima, *Chem. Lett.*, 1998, 691; I. A. Fallis, R. D. Farley, K. M. A. Malik, D. M. Murphy and H. J. Smith, *J. Chem. Soc., Dalton Trans.*, 2000, 3632; D. A. Leigh, P. J. Lusby, S. J. Teat, A. J. Wilson and J. K. Y. Wong, *Angew. Chem., Int. Ed.*, 2001, **40**, 1538; D. Martini, M. Pellei, C. Pettinari, B. W. Skelton and A. H. White, *Inorg. Chim. Acta*, 2002, **333**, 72.
56 G. Wingefeld and R. Hoppe, *Z. Anorg. Allg. Chem.*, 1984, **516**, 223.
57 M. Atanasov, M. A. Hitchman, R. Hoppe, K. S. Murray, B. Moubaraki, D. Reinen and H. Stratemeier, *Inorg. Chem.*, 1993, **32**, 3397.
58 V. M. Masters, M. J. Riley and M. A. Hitchman, *J. Synchrotron Radiat.*, 1999, **6**, 242.
59 P. Fischer, W. Hälg, D. Schwartzenbach and W. Gamsjäger, *J. Phys. Chem. Solids*, 1974, **35**, 1683.
60 V. Kaiser, M. Otto, F. Binder and D. Babel, *Z. Anorg. Allg. Chem.*, 1990, **585**, 93.
61 R. W. Buttner, E. W. Maslen and W. Spadaccini, *Acta Crystallogr., Sect. B*, 1990, **46**, 131; M. Hidaka, T. Eguchi and I. Yamada, *J. Phys. Soc. Jpn.*, 1998, **67**, 2488.
62 D. Babel and M. Otto, *Z. Naturforsch., Teil B*, 1989, **44**, 715.
63 R. Haegele and D. Babel, *Z. Anorg. Allg. Chem.*, 1974, **409**, 11.
64 E. Herdtweck and D. Babel, *Z. Anorg. Allg. Chem.*, 1981, **474**, 113.
65 D. Reinen and S. Krause, *Inorg. Chem.*, 1981, **20**, 2750.
66 P. Núñez, M. Morales-Escobar, T. Roisnel, J. M. Kiat, R. Saez-Puche, H. Guengard, J. Grannec and A. Tressaud, *J. Solid State Chem.*, 1996, **122**, 87.
67 J. Renaudin, M. LeBlanc, G. Ferey, A. De Kozack and M. Samouel, *J. Solid State Chem.*, 1988, **73**, 603.
68 S. Llorente, F. Goubard, P. Gredin, D. Bizot, J. Chassaing and M. Quarton, *Z. Anorg. Allg. Chem.*, 1998, **624**, 1538.
69 B. G. Müller, *Z. Anorg. Allg. Chem.*, 1988, **556**, 79.
70 F. Schrötter and B. G. Müller, *Z. Kristallogr.*, 1991, **196**, 261.
71 K. Knox, *J. Chem. Phys.*, 1959, **30**, 991.
72 L. Basso, A. Palenzona and L. Zefiro, *Neues Jahrb. Mineral. Monatsh.*, 1988, 385; M. A. Lafontaine, A. Le Bail and G. Ferey, *J. Solid State Chem.*, 1990, **85**, 220.
73 H. Effenberger, *Z. Kristallogr.*, 1989, **188**, 43.
74 M. Gruss and R. Glaum, *Z. Kristallogr.*, 1997, **212**, 510.
75 U. Steiner and W. Reichelt, *Acta Crystallogr., Sect. C*, 1997, **53**, 1371.
76 M. E. Fleet, *Acta Crystallogr., Sect. B*, 1975, **31**, 183.
77 J. D. Grice, J. T. Szymanski and J. L. Jambor, *Can. Mineral.*, 1996, **34**, 73.
78 R. Cousin, S. Capelle, E. Abi-Aad, D. Courcot and A. Aboukais, *Chem. Mater.*, 2001, **13**, 3862.
79 F. Hanic and A. Cakajdová, *Acta Crystallogr.*, 1958, **11**, 610.
80 F. Hanic, *Acta Crystallogr.*, 1959, **12**, 739.
81 L. Zsoldos, *Magy. Fiz. Foly.*, 1962, **10**, 189.
82 B. Papánková, M. Serátor, J. Gazo and J. Stracelsky, *Inorg. Chim. Acta*, 1982, **60**, 171.
83 J. Kohout and J. Gazo, *Chem. Zvesti*, 1968, **22**, 905.
84 T. Obert and I. B. Bersuker, *Czech. J. Phys. B*, 1983, **33**, 568.
85 J. Gazo, I. B. Bersuker, J. Garaj, M. Kabesová, J. Kohout, H. Langfelderová, M. Melník, M. Serátor and F. Valach, *Coord. Chem. Rev.*, 1976, **19**, 253.
86 J. P. Steadman and R. D. Willett, *Inorg. Chim. Acta*, 1970, **4**, 367.
87 Y. Moritomo and Y. Tokura, *J. Chem. Phys.*, 1994, **101**, 1763.
88 B. A. Moral and F. Rodriguez, *J. Phys. Chem. Solids*, 1997, **58**, 1487; B. A. Moral, F. Rodriguez, R. Valiente, M. Moreno and H. U. Gudel, *Z. Phys. Chem.*, 1997, **201**, 425; R. Valiente, F. Rodriguez, M. T. Bariuso, J. A. Aramburu and M. Moreno, *Radiat. Eff. Def. Solids*, 1999, **151**, 1097.
89 R. Valiente, F. Rodriguez, M. Moreno and L. Lezama, *NATO Sci. Ser., II Math., Phys. Chem.*, 2001, **39**, 221.
90 C. J. Simmons, M. A. Hitchman, H. Stratemeier and A. J. Schulz, *J. Am. Chem. Soc.*, 1993, **115**, 11304; W. Rauw, H. Ahsbahs, M. A. Hitchman, S. Lukin, D. Reinen, A. J. Schulz, C. J. Simmons and H. Stratemeier, *Inorg. Chem.*, 1996, **35**, 1902; A. J. Schulz, M. A. Hitchman, J. D. Jorgenson, S. Lukin, P. G. Radaelli, C. J. Simmons and H. Stratemeier, *Inorg. Chem.*, 1997, **36**, 3382.
91 W. R. Clayton and E. A. Meyers, *Cryst. Struct. Commun.*, 1976, **5**, 57; W. R. Clayton and E. A. Meyers, *Cryst. Struct. Commun.*, 1976, **5**, 61; W. R. Clayton and E. A. Meyers, *Cryst. Struct. Commun.*, 1976, **5**, 63; F. Valach, M. Dunaj-Jurco, M. Serátor and V. Jonk, *Z. Kristallogr.*, 1994, **209**, 343.
92 B. E. Billing, B. J. Hathaway and A. A. G. Tomlinson, *J. Chem. Soc. A*, 1971, 2839.
93 M. J. Riley, M. A. Hitchman, D. Reinen and G. Steffen, *Inorg. Chem.*, 1988, **27**, 1924.
94 G. Steffen, U. Kaschuba, M. A. Hitchman and D. Reinen, *Z. Naturforsch., Teil B*, 1992, **47**, 465.
95 J. A. C. van Ooijen, P. J. van der Put and J. Reedijk, *Chem. Phys. Lett.*, 1977, **51**, 380.
96 C. H. McGillavry and J. M. Bijvoet, *Z. Kristallogr.*, 1936, **94**, 231.
97 S. Gorter, A. D. van Ingen Schenau and G. C. Verschoor, *Acta Crystallogr., Sect. B*, 1974, **30**, 1867; this manuscript describes the structure of $[MnCl_2(pz)_2]$, which is isomorphous with the Cd compound.[95].
98 E. Herdtweck and D. Babel, *Z. Kristallogr.*, 1980, **153**, 189.
99 O. A. Amkeenov, R. M. Gumerov, M. V. Eremin, T. A. Ivanova and Yu. V. Yablokov, *Solid State Phys.*, 1984, **26**, 2249; M. A. Hitchman, R. G. McDonald and D. Reinen, *Inorg. Chem.*, 1986, **25**, 519.
100 C. Freibel, V. Propach and D. Reinen, *Z. Naturforsch., Teil B*, 1976, **31**, 1574; G. Steffen, D. Reinen, H. Stratemeier, M. J. Riley, M. A. Hitchman, H. E. Matthies, K. Recker, F. Wallrafen and J. R. Niklas, *Inorg. Chem.*, 1990, **29**, 2123.
101 H. G. von Schnering, *Z. Anorg. Allg. Chem.*, 1967, **353**, 13.
102 X.-Y. Kuang and K.-W. Zhou, *Physica B*, 2001, **307**, 34, and references therein.
103 C. Friebel and D. Reinen, *Z. Anorg. Allg. Chem.*, 1974, **407**, 193.
104 R. W. Reynolds, L. A. Boatner, M. M. Abraham and Y. Chen, *Phys. Rev. B*, 1974, **10**, 3802.
105 S. Guha and L. L. Chase, *Phys. Rev. Lett.*, 1974, **32**, 869; S. Guha and L. L. Chase, *Phys. Rev. B*, 1975, **12**, 1658.
106 C. E. Housecroft and A. G. Sharpe, *Inorganic Chemistry*, Prentice Hall, Harlow, 2001, Appendix 6, pp. 744–745.
107 A. Raizman, J. Barak, R. Englman and J. T. Suss, *Phys. Rev. B*, 1981, **24**, 6262.
108 M. Winkelmann, H. A. Graf, B. Wagner and A. W. Hewat, *Z. Kristallogr.*, 1994, **209**, 870.
109 A. B. Vassilikou-Dova and K. Eftaxias, *J. Phys. Condens. Matter*, 1992, **4**, 241.
110 J. Chandrasekhar and S. Subramanian, *J. Magn. Reson.*, 1974, **16**, 82.
111 F. Köksal, I. Kartal and A. Gençten, *Z. Naturforsch., Teil A*, 1998, **53**, 779.
112 N. K. Solanki, E. J. L. McInnes, F. E. Mabbs and M. A. Halcrow, unpublished data.
113 N. K. Solanki, E. J. L. McInnes, D. Collison, C. A. Kilner, J. E. Davies and M. A. Halcrow, *J. Chem. Soc., Dalton Trans.*, 2002, 1625.
114 M. A. Halcrow, C. A. Kilner and M. Thornton-Pett, *Acta Crystallogr., Sect. C*, 2000, **56**, 213.
115 J. M. Holland, S. A. Barrett, C. A. Kilner and M. A. Halcrow, *Inorg. Chem. Commun.*, 2002, **5**, 328.
116 A. T. Baker, D. C. Craig, G. Dong and A. D. Rae, *Aust. J. Chem.*, 1995, **48**, 1071.
117 M. A. Halcrow, C. A. Kilner, J. Wolowska, E. J. L. McInnes and A. J. Bridgeman, *New J. Chem.*, DOI: 10.1039/ b309071j.
118 D. A. Fletcher, R. F. McMeeking and D. Parkin, *J. Chem. Inf. Comput. Sci.*, 1996, **36**, 746.